Cytochrome *P*450 Epoxygenase Promotes Human Cancer Metastasis

Jian-Gang Jiang,[1] Yao-Gui Ning,[1] Chen Chen,[1] Ding Ma,[1] Zhen-Jun Liu,[1] Shilin Yang,[1] Jianfeng Zhou,[1] Xiao Xiao,[1,2] Xin A. Zhang,[3] Matthew L. Edin,[4] Jeffrey W. Card,[4] Jianing Wang,[1] Darryl C. Zeldin,[4] and Dao Wen Wang[1]

[1]The Institute of Hypertension and Department of Internal Medicine, Tongji Hospital, Tongji Medical College, Huazhong University of Science and Technology, Wuhan, People's Republic of China; [2]Molecular Pharmaceutics, University of North Carolina School of Pharmacy, Chapel Hill, North Carolina; [3]Vascular Biology Center and Department of Medicine and Department of Molecular Science, University of Tennessee Health Science Center, Memphis, Tennessee; and [4]Division of Intramural Research, National Institute of Environmental Health Sciences, NIH, Research Triangle Park, North Carolina

Abstract

Cytochrome *P*450 (CYP) epoxygenases convert arachidonic acid to four regioisomeric epoxyeicosatrienoic acids (EET), which exert diverse biological activities in a variety of systems. We previously reported that the CYP2J2 epoxygenase is overexpressed in human cancer tissues and cancer cell lines and that EETs enhance tumor growth, increase carcinoma cell proliferation, and prevent apoptosis of cancer cells. Herein, we report that CYP epoxygenase overexpression or EET treatment promotes tumor metastasis independent of effects on tumor growth. In four different human cancer cell lines *in vitro*, overexpression of CYP2J2 or CYP102 F87V with an associated increase in EET production or addition of synthetic EETs significantly induced Transwell migration (4.5- to 5.5-fold), invasion of cells (3- to 3.5-fold), cell adhesion to fibronectin, and colony formation in soft agar. In contrast, the epoxygenase inhibitor 17-ODYA or infection with the antisense recombinant adeno-associated viral vector (rAAV)-CYP2J2 vector inhibited cell migration, invasion, and adhesion with an associated reduction in EET production. CYP overexpression also enhanced metastatic potential *in vivo* in that rAAV-CYP2J2–infected MDA-MB-231 human breast carcinoma cells showed 60% more lung metastases in athymic BALB/c mice and enhanced angiogenesis in and around primary tumors compared with control cells. Lung metastasis was abolished by infection with the antisense rAAV-CYP2J2 vector. CYP epoxygenase overexpression or EET treatment up-regulated the prometastatic matrix metalloproteinases and CD44 and down-regulated the antimetastatic genes *CD82* and *nm-23*. Together, these data suggest that CYP epoxygenase inhibition may represent a novel approach to prevent metastasis of human cancers. [Cancer Res 2007;67(14):6665–74]

Introduction

Cytochrome *P*450 (CYP) epoxygenases metabolize arachidonic acid to biologically active eicosanoids termed *cis*-epoxyeicosatrienoic acids (5,6-EET, 8,9-EET, 11,12-EET, and 14,15-EET; ref. 1). Early studies identified EETs as endothelium-derived hyperpolarizing factors, which activate calcium-sensitive potassium channels to result in hyperpolarization of resting membrane potential and relaxation of vascular smooth muscle cells (2). Subsequent work has shown that EETs have diverse biological effects within the cardiovascular system. Addition of EETs or CYP2J2 overexpression diminishes cytokine-induced endothelial cell adhesion molecule expression and inhibits leukocyte adhesion to vessel walls (3). These effects involve suppression of NF-κB and IκB kinase and suggest that EETs have anti-inflammatory effects independent of membrane hyperpolarization (3). We have observed that EETs up-regulate endothelial nitric oxide synthase (4) and stimulate endothelial cell proliferation and angiogenesis via activating both mitogen-activated protein kinase (MAPK) and phosphatidylinositol 3-kinase (PI3K)/Akt signaling pathways (5). Addition of synthetic EETs or CYP2J2 overexpression protects endothelial cells against hypoxia-reoxygenation injury *in vitro* (6) and shows fibrinolytic effects by increasing tissue plasminogen activator (t-PA) expression and activity (7). CYP2J2 overexpression and addition of synthetic EETs also protect against post-ischemic myocardial dysfunction through activating mitochondrial ATP-sensitive K^+ channels and the MAPK pathway (8). Collectively, these data describe a role for CYP2J2-derived EETs in cardiovascular protection.

However, in a recent publication, we described potentially deleterious effects of CYP2J2 expression and EET biosynthesis. Elevated CYP2J2 mRNA and protein levels were found in a set of diverse human-derived cancer cell lines and human cancer tissues but not in noncancer cell lines or adjacent normal tissues (9). Addition of exogenous EETs or recombinant adeno-associated viral vector (rAAV)-mediated delivery of CYP2J2 or CYP102 F87V (a selective 14,15-EET epoxygenase) markedly promoted proliferation of cancer cells *in vitro* and *in vivo*. In neoplastic cell lines, epoxygenase overexpression or EET addition increased activation of MAPK and PI3K/Akt pathways and enhanced phosphorylation of epidermal growth factor receptor (EGFR). EETs also inhibited carcinoma cell apoptosis through up-regulation of the antiapoptotic proteins Bcl-2 and Bcl-xL and down-regulation of the proapoptotic protein Bax (9). These results suggested that the CYP2J2 epoxygenase plays a previously unrecognized role in the promotion of the neoplastic phenotype and in the pathogenesis of a variety of human cancers.

The roles of CYP-derived EETs in carcinoma cell metastasis have yet to be examined. Herein, we show that CYP epoxygenase overexpression or EET treatment markedly enhanced the migration, invasion, and prometastatic gene expression profiles in a variety of cancer cell lines *in vitro*. In addition, CYP epoxygenase overexpression enhanced tumor metastasis of MDA-MB-231 human breast carcinoma cells to lungs of athymic BALB/C mice.

Note: Supplementary data for this article are available at Cancer Research Online (http://cancerres.aacrjournals.org/).

J-G. Jiang and Y-G. Ning contributed equally to this work.

Requests for reprints: Dao Wen Wang, Department of Internal Medicine, Tongji Hospital, Tongji Medical College, Huazhong University of Science and Technology, 1095 Jiefang Avenue, Wuhan 430030, People's Republic of China. Phone: 86-27-8366-2842; Fax: 86-27-8366-2842; E-mail: dwwang@tjh.tjmu.edu.cn.

doi:10.1158/0008-5472.CAN-06-3643

These data describe a previously unrecognized role for EETs in the promotion of carcinoma metastasis and may have important therapeutic implications.

Materials and Methods

The human breast cancer cell lines MDA-MB-231, Tca-8113, A549, Hcl-H446, and HepG2 were obtained from the American Type Culture Collection and maintained as recommended. Chemicals and reagents were obtained as follows: cell culture medium and Trizol reagent from Life Technologies; antibodies against nm-23, CD44, KAI-1/CD82, matrix metalloproteinase (MMP)-2, and MMP-9 from Santa Cruz Biotechnology, Inc.; antibodies against human E-cadherin from Cell Signaling Technology; antibody against β-actin from NeoMarkers; horseradish peroxidase (HRP)-conjugated secondary antibodies (goat anti-rabbit IgG and rabbit anti-mouse IgG) from KPL; enhanced chemiluminescence reagents from Pierce, Inc.; polyvinylidene difluoride (PVDF) membranes, prestained protein markers, and SDS-PAGE gels from Bio-Rad, Inc.; and synthetic 8,9-EET, 11,12-EET, and 14,15-EET from Sigma Chemical Co. Polyclonal antibodies against CYP2J2 were developed as described (10) and showed no cross-reactivity with other *P*450 isoforms. Antibody against CYP102 F87V was a kind gift from Dr. Jorge Capdevila (Vanderbilt University Medical School, Nashville, TN). All other reagents were purchased from standard commercial suppliers unless otherwise specified.

Cell culture, infection with rAAV, incubation with EETs, and determination of 14,15-dihydroxyeicosatrienoic acid levels. Tca-8113, A549, Hcl-H446, and HepG2 cells were cultured in DMEM with 10% fetal bovine serum (FBS) at 37°C in a 95% air/5% CO_2 at constant humidity. MDA-MB-231 cells were grown in RPMI 1640 with 10% FBS. For some experiments, cells were infected with rAAV-CYP2J2, rAAV-CYP102 F87V, rAAV-antisense-CYP2J2, or rAAV-GFP (~100 virons per cell), packed and purified as described previously (11, 12), and grown for 1 week before use. Cells were grown to 60% confluence, the medium was removed, and the cells were washed thrice with PBS. Cells were incubated with serum-free medium at 37°C for 12 h to allow for synchronization. Cells were treated with vehicle (ethanol), 8,9-EET, 11,12-EET, and 14,15-EET (100 nmol/L each) or left untreated, as indicated, for migration, invasion, or adhesion studies.

For measurement of EETs and dihydroxyeicosatrienoic acid in the cultured cells, the cells infected with the different rAAVs for 7 days in 150-mm dishes were scraped in cold PBS (pH 7.2) with triphenylphosphine after washing with PBS and then homogenized and sonicated over ice. Eicosanoids were extracted from the cell homogenates thrice with ethyl acetate after acidification with acetic acid. After evaporation, the samples were dissolved in *N*,*N*-dimethylformamide (Amresco) and concentrations of the stable EET metabolite 14,15-dihydroxyeicosatrienoic acid (DHET) were determined by an ELISA kit (Detroit R&D) according to the manufacturer's instructions. Results were expressed as nanograms of DHET per 250 μg proteins.

Cell migration and invasion assays. Chemotactic migration was evaluated using a modified Boyden chamber as described (13). Porous filters (8-μm pores) were coated by passive adsorption for 24 h with type IV collagen (10 μg/mL collagen in coating buffer; Sigma). Cells (1×10^5) were plated in the upper chamber. The bottom chamber contained 5% FBS-supplemented medium as a chemoattractant. Subsequently, serum-free medium with individual EETs (100 nmol/L) was added to the upper chamber and cells were allowed to migrate for 5 h. Nonmigrating cells were removed from the upper chamber with a cotton swab and filters were stained with DiffQuik stain. Migrating cells adherent to the underside of the filter were counted with an ocular micrometer, counting a minimum of 10 high-powered fields (HPF). To study cell invasiveness, rAAV-infected or EET-treated cells (5×10^4) were plated onto Boyden chambers coated with Matrigel (500 μg/filter) and incubated for 48 to 72 h. Chambers were stained as described above and invasiveness was evaluated by quantifying the number of cells invading the Matrigel and reaching the opposite side of the filter. To test whether EET-induced up-regulation and activation of MMPs play a role in EET-enhanced migration and invasion, 11,12-EET–treated cells (100 nmol/L) were incubated with nonspecific MMP inhibitor 1,10-phenanthrolin (100 μmol/L) for 6 h and then migration and invasiveness were evaluated as described above. All the data are expressed as relative migration (number of cells per field) and represent the mean ± SE of quadruplicate experiments.

Injection of MDA-MB-231 cells and lung colony measurement. All animal studies were approved by the Animal Research Committee of Tongji Medical College and done according to guidelines set forth by the NIH. Athymic BALB/c mice, 4 weeks of age, were housed on a 12-h light/12-h dark cycle in a pathogen-free environment and allowed *ad libitum* access to food and water. MDA-MB-231 cells were cultured and infected with rAAV-CYP2J2, rAAV-antisense-CYP2J2, and rAAV-GFP (~100 virons per cell) as described above. One week after infection, the cells (5×10^6 in 0.4 mL of phosphate buffer solution) were inoculated into the mammary fat pads of female athymic BALB/C mice ($n = 8$ for each group). Tumor size was measured once every 5 days (beginning 7 days after injection) with microcalipers. Tumor volumes were calculated as length × width^2 × 0.5236 as described previously (14). At the end of the experiment (14 weeks after cell injection), mice were sacrificed by sodium pentobarbital overdose (90 mg/kg i.p.), and primary tumors were removed, weighed, and analyzed for protein expression. Lungs were also removed for quantification of white metastatic colonies on the lung surfaces.

Two additional experiments were done to exclude the effects of differential xenograft tumor proliferation on metastasis into lungs. Cells were infected and inoculated into the mammary fat pads of female athymic BALB/C mice as described above. These mice were monitored and tumors were measured until the primary xenograft tumors reached a volume of ~2.5 cm^3. The animals were subsequently euthanized and autopsied. Primary xenograft tissues were weighed and white metastatic colonies on the lung surfaces were counted ($n = 6$ for each group). In a separate experiment, lung metastasis was assessed after MDA-MB-231 cells infected with either rAAV-GFP, rAAV-CYP2J2, or rAAV-antisense-CYP2J2 (5×10^5 in 0.3 mL DMEM) were injected into mouse tail veins according to methods previously described (15) and the animals were sacrificed at 4 weeks to evaluate lung metastases as described above ($n = 6$ for each group).

We also evaluated the effects of CYP2J2 overexpression on angiogenesis in and around xenograft tumors as the method described by Weidner et al. (16) Briefly, xenograft tumors were sectioned and stained using anti-CD31 antibodies. The areas of invasive tumor containing the highest numbers of capillaries and small venules per area ("hotspots") were selected by light microscopy at low magnification (×40). After the area of highest neovascularization was identified, individual microvessel counts were made on a 200× field. Results were expressed as the mean value of all the fields.

To confirm if the carcinoma-enhancing effect is CYP2J2 mediated, we did 3-(4,5-dimethylthiazol-2-yl)-2,5-diphenyltetrazolium bromide (MTT) assays using the selective CYP2J2 inhibitor WL-01 (a terfinadine derivative; 5 or 10 μmol/L; ref. 17) with or without 11,12-EET (100 nmol/L).

MMP-2 and MMP-9 gelatin zymography. MMP-2 and MMP-9 gelatin zymography was carried out according to previously published methods (18). Briefly, samples containing equal amounts of protein were subjected to 10% nonreducing SDS-PAGE (containing 0.1% gelatin). After electrophoresis, the gels were washed with 2.5% Triton X-100 for 30 min and with developing buffer (10 mmol/L Tris base, 40 mmol/L Tris-HCl, 200 mmol/L NaCl, 5 mmol/L $CaCl_2$, 0.02% Briji35) for 1 h. After washing, the gels were incubated with fresh developing buffer overnight at 37°C. The gels were then stained with Coomassie solution (0.5% Coomassie blue in 10% methanol, 5% acetic acid) for 1 h and destained with 10% methanol and 5% acetic acid.

Colony formation assay. Soft agar colony formation assays were done in six-well dishes as described previously (19). Briefly, cells (2.5×10^3) infected with either rAAV-CYP2J2, rAAV-GFP, or rAAV-antisense-CYP2J2 were suspended in 1.5 mL of 0.3% bactoagar with growth medium (RPMI 1640 supplemented with 10% FBS). Cells were added to a base layer of 0.6% bactoagar containing culture medium and incubated at 37°C in a 5% CO_2 incubator for 2 weeks. Colony formation was assessed by counting the number of colonies under low magnification (×100) at four points on each well. A colony was defined as >10 cells in one site.

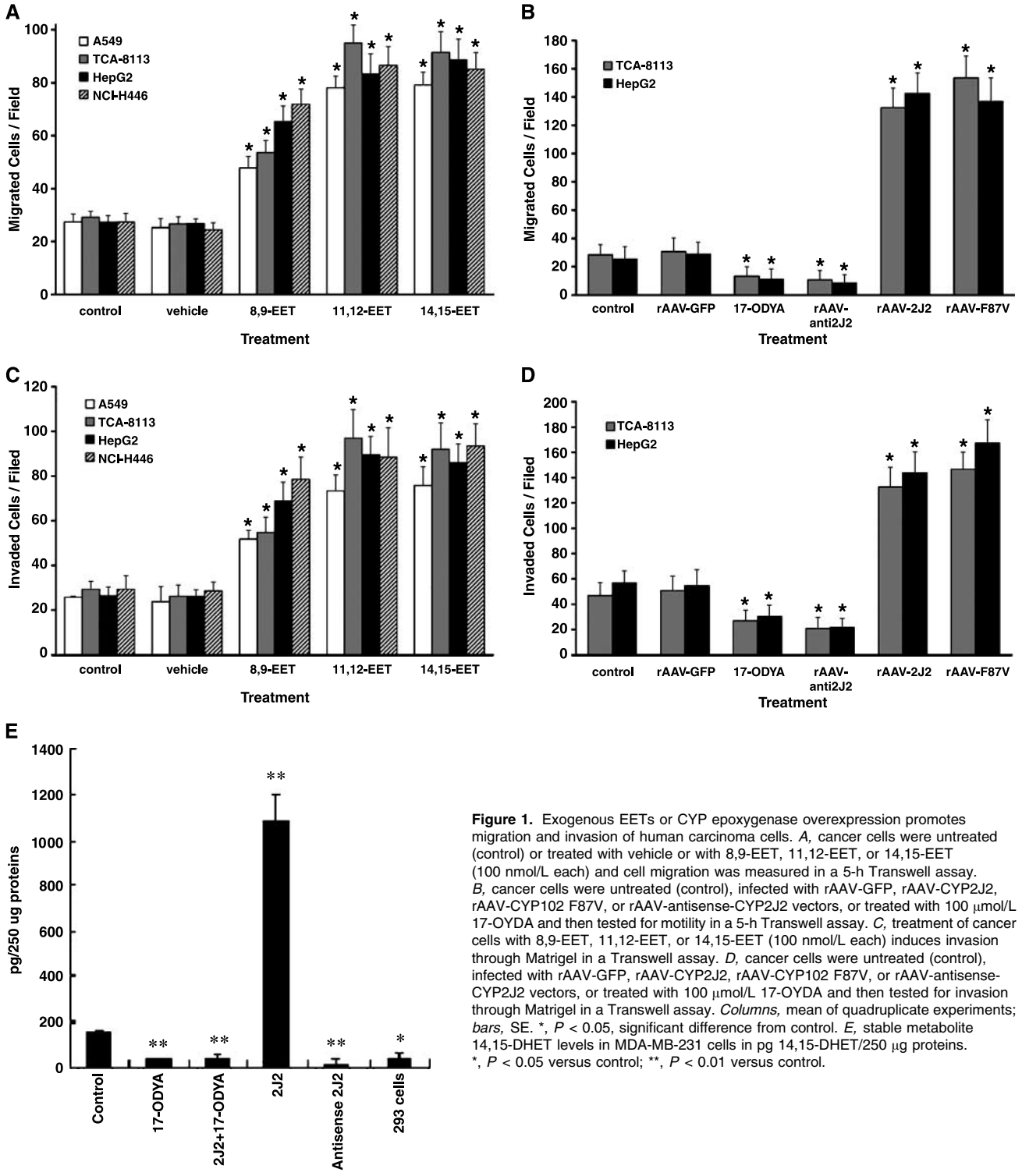

Figure 1. Exogenous EETs or CYP epoxygenase overexpression promotes migration and invasion of human carcinoma cells. *A,* cancer cells were untreated (control) or treated with vehicle or with 8,9-EET, 11,12-EET, or 14,15-EET (100 nmol/L each) and cell migration was measured in a 5-h Transwell assay. *B,* cancer cells were untreated (control), infected with rAAV-GFP, rAAV-CYP2J2, rAAV-CYP102 F87V, or rAAV-antisense-CYP2J2 vectors, or treated with 100 μmol/L 17-OYDA and then tested for motility in a 5-h Transwell assay. *C,* treatment of cancer cells with 8,9-EET, 11,12-EET, or 14,15-EET (100 nmol/L each) induces invasion through Matrigel in a Transwell assay. *D,* cancer cells were untreated (control), infected with rAAV-GFP, rAAV-CYP2J2, rAAV-CYP102 F87V, or rAAV-antisense-CYP2J2 vectors, or treated with 100 μmol/L 17-OYDA and then tested for invasion through Matrigel in a Transwell assay. *Columns,* mean of quadruplicate experiments; *bars,* SE. *, $P < 0.05$, significant difference from control. *E,* stable metabolite 14,15-DHET levels in MDA-MB-231 cells in pg 14,15-DHET/250 μg proteins. *, $P < 0.05$ versus control; **, $P < 0.01$ versus control.

Fibronectin adhesion assay. Adhesion of cells to fibronectin was carried out as described previously (20). Briefly, nontissue culture 96-well plates were coated with 100 μL/well of 10 μg/mL fibronectin for 60 min at 37°C and blocked twice with 200 μL of 1% bovine serum albumin (BSA) in RPMI 1640 for 30 min at 37°C. Three wells were not coated to determine nonspecific binding. Cells (1×10^4 in 100 μL RPMI 1640 containing 0.1% BSA) infected with or without rAAV-GFP, rAAV-antisense-CYP2J2, or rAAV-CYP2J2 were added to fibronectin-coated wells for 60 min at 37°C. Noninfected cells were adhered in the presence or absence of 100 nmol/L EETs as indicated. After three washes with medium to remove nonadhered cells, the cells were covered with 100 μL RPMI 1640 and 20 μL MTT solution (5 mg/mL) was added for cell viability analysis (9). Absorbance

values at 570 nm reflect the proportional number of cells adhering to fibronectin.

Immunoblot analysis of nm-23, CD44, KAI-1/CD82, MMP-2, MMP-9, and CYP2J2 expression. Proteins were extracted from xenograft tumors and rAAV-infected or EET-treated cells with Trizol reagent for immunoblot analysis. Protein concentration was determined by Bradford method and 20 μg of protein extract were subjected to electrophoresis in 8% polyacrylamide slab gels and transferred to PVDF membrane, blocked with 5% nonfat milk, and probed with nm-23, CD44, KAI-1/CD82, MMP-2, MMP-9, and CYP2J2 antibodies (1:750 dilution). Blots were washed, incubated with HRP-conjugated secondary antibody (rabbit anti-goat at 1:800 dilution), and visualized by enhanced chemiluminescence.

Statistical analysis. Student's *t* test was used for statistical analysis of all migration and invasion assays as well as for the analysis of xenograft tumor volume and metastases. Each experiment was done at least in triplicate. Results are expressed as mean ± SE of the mean. A P value of <0.05 was taken as the level of significance for all tests.

Results

CYP epoxygenase–derived EETs enhance migration and invasion of carcinoma cells. We previously showed that the human cancer cell lines Tca-8113, A549, HepG2, NCl-H446, LS-174, SiHa, U251, and ScaBER have abundant CYP2J2 expression, whereas the noncancer cell lines HEK293 and HT1080 do not (9). Four representative cell lines (Tca-8113, A549, Hcl-H446, and HepG2) were used in the current studies. We previously showed that infection of these four cell lines with rAAV-CYP2J2 or rAAV-CYP102 F87V resulted in increased expression of the respective recombinant proteins, whereas infection with rAAV-antisense-CYP2J2 resulted in reduced CYP2J2 expression compared with control cells infected with rAAV-GFP or uninfected cells (9). Addition of 100 nmol/L of each EET regioisomer significantly increased cell migration in all four carcinoma cell lines examined in the Transwell assay (2- to 4.5-fold increase over control; Fig. 1*A*). Similarly, infection with rAAV-CYP2J2 or rAAV-CYP102 F87V significantly increased Tca-8113 and HepG2 Transwell migration 5- to 6-fold above control levels (Fig. 1*B*). In contrast, treatment with the CYP epoxygenase inhibitor 17-ODYA or infection with rAAV-antisense-CYP2J2 significantly inhibited migration compared with control (Fig. 1*B*). Moreover, infection with rAAV-CYP2J2 or rAAV-CYP102 F87V or the addition of EET regioisomers significantly promoted invasion of carcinoma cells into Matrigel to levels that were 2- to 4-fold above control levels (Fig. 1*C*). Invasion was attenuated by addition of the CYP epoxygenase inhibitor 17-ODYA or infection with rAAV-antisense-CYP2J2 (Fig. 1*D*). Together, these results indicate that CYP epoxygenase–derived EETs enhance migration and invasion of human carcinoma cells *in vitro*.

To investigate the functional role of the CYP2J2 in the cancer cells, we measured the concentration of the major CYP2J2 epoxidation product of arachidonic acid. Given the instability of 14,15-EET, we determined the concentration of its stable metabolite, 14,15-DHET, after extraction from cell homogenates. 14,15-DHET levels were significantly higher in rAAV-2J2–transfected cells (1,078.67 ± 124.42 ng/250 μg protein in rAAV-CYP2J2 versus 156.67 ± 9.45 ng/10^5 cells in blank; $P < 0.01$). In contrast, the epoxygenase inhibitor 17-ODYA or infection with the antisense rAAV-CYP2J2 markedly decreased 14,15-DHET levels compared with control ($P < 0.01$; Fig. 1*E*).

CYP2J2-derived EETs enhance migration of MDA-MB-231 breast carcinoma cells. MDA-MB-231 cells are a model cell line to study breast tumor metastasis in mice (21). To confirm efficiency of rAAV-mediated epoxygenase gene transfer and long-term expression of CYP epoxygenases in MDA-MB-231 cells, we analyzed cells *in vitro* before injection and in xenograft tumors grown *in vivo* for 14 weeks in athymic BALB/c mice. MDA-MB-231 cells have elevated CYP2J2 protein levels compared with HEK293 cells (Fig. 2*A*). One week after infection of MDA-MB-231 cells with rAAV-CYP2J2, we observed increased CYP2J2 expression compared with uninfected or rAAV-GFP–infected controls (Fig. 2*A*). In contrast, infection of MDA-MB-231 cells with rAAV-antisense-CYP2J2 resulted in reduced CYP2J2 expression (Fig. 2*A*). Similarly, protein extracts from mouse xenograft tumors confirmed that

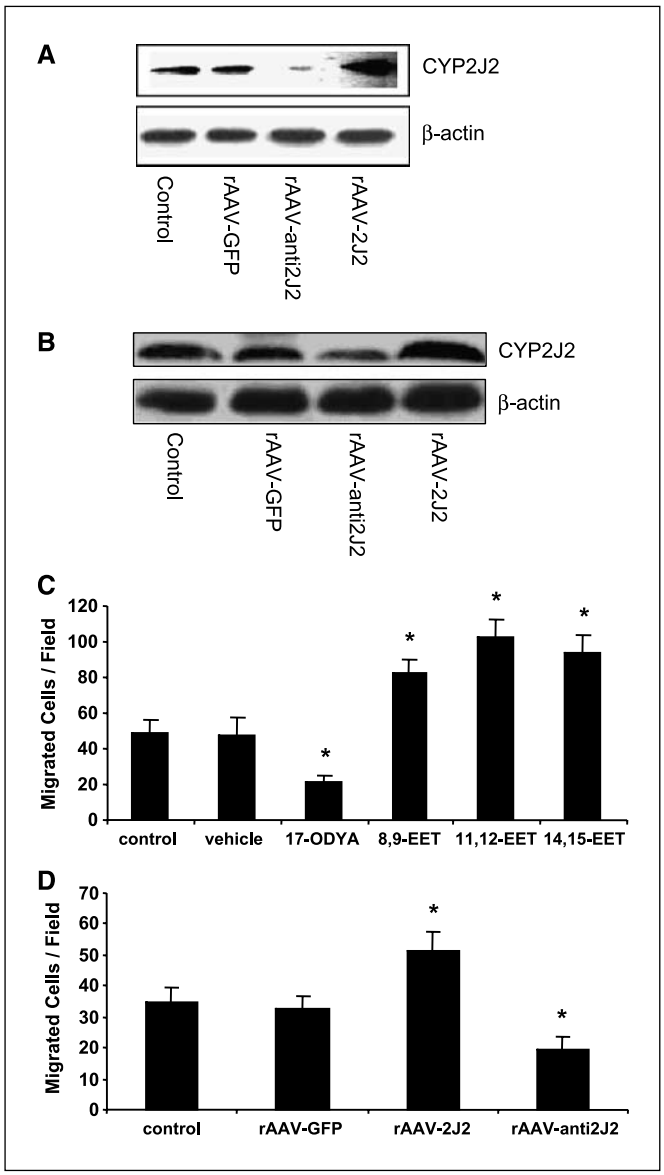

Figure 2. CYP2J2-derived EETs enhance migration in MDA-MB-231 cancer cells. *A,* expression of CYP2J2 and β-actin protein in HEK293 cells or MDA-MB-231 cells without infection (control) or 1 wk after infection with rAAV-GFP, rAAV-CYP2J2, or rAAV-antisense-CYP2J2. *B,* expression of CYP2J2 and β-actin protein in xenograft tumors in mice 14 wks following injection of infected MDA-MB-231 cells. *C,* MDA-MB-231 cells were treated with vehicle, 100 μmol/L 17-ODYA, or 8,9-EET, 11,12-EET, or 14,15-EET (100 nm each) and tested for migration in a 5-h Transwell assay. *D,* uninfected MDA-MB-231 cells (control) or MDA-MB-231 cells infected with rAAV-GFP, rAAV-CYP2J2, or rAAV-antisense-CYP2J2 were tested for migration in a 5-h Transwell assay. *Columns,* mean of quadruplicate experiments; *bars,* SE. *, $P < 0.05$, significant difference from control.

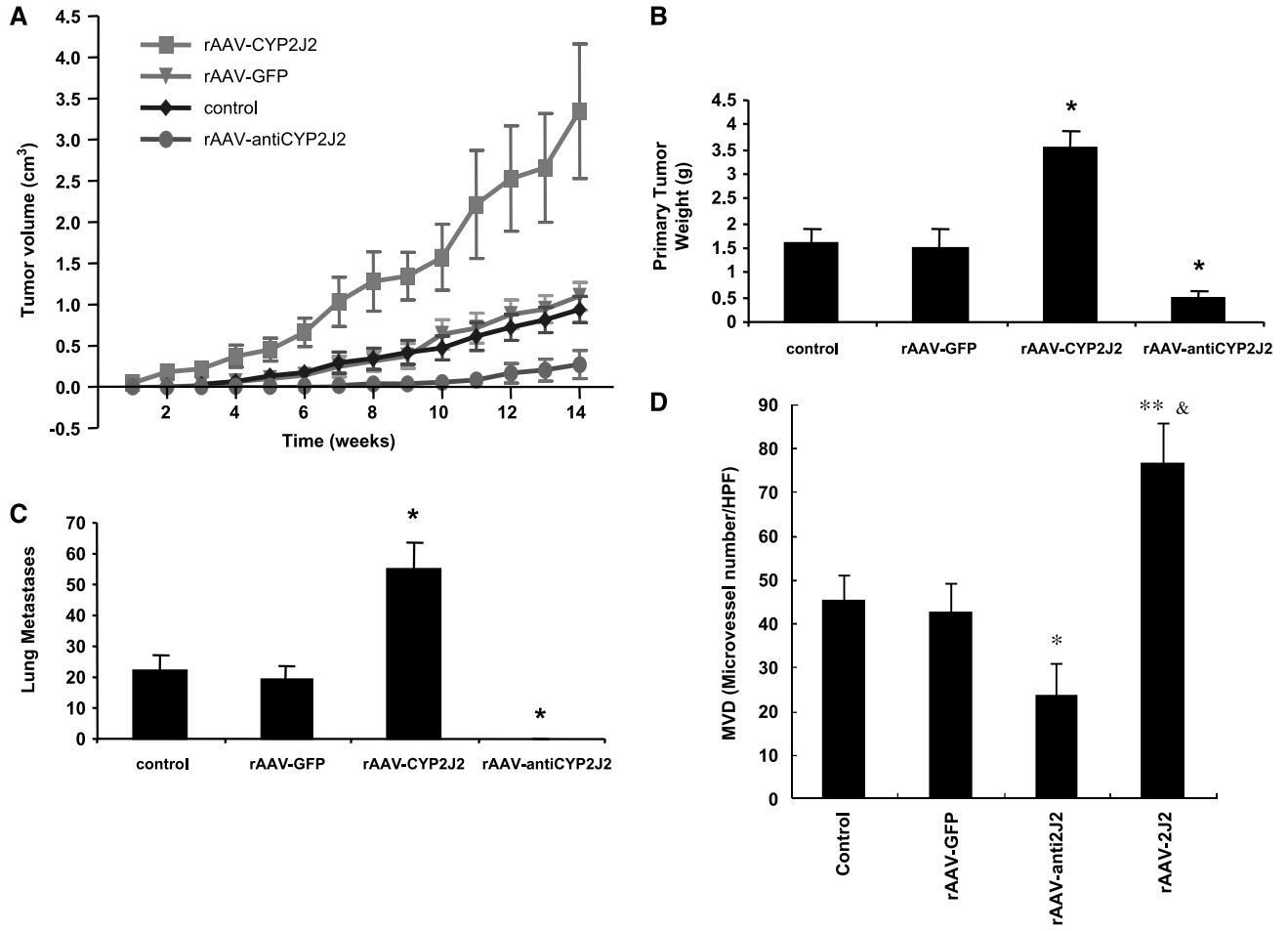

Figure 3. rAAV-mediated CYP2J2 overexpression in MDA-MB-231 cells promotes primary tumor growth and metastasis to lungs in mice. *A,* primary xenograft tumor volume growth curves in mice injected with uninfected MDA-MB-231 cells (control) or cells infected with rAAV-GFP, rAAV-CYP2J2, or rAAV-antisense-CYP2J2. *B,* average primary tumor weight for each group after growth for 14 wks. *C,* average number of lung metastases for each group. *Columns,* mean; *bars,* SE. *, $P < 0.01$ versus control. *D,* average microvessel density (*MVD*; capillary vessel number per HPF) in primary tumors and around tumors. *, $P < 0.05$ versus control and rAAV-GFP; ** and &, $P < 0.01$ versus control or rAAV-GFP and rAAV-antisense-CYP2J2, respectively. *E,* readings of MTT assays showing effect of CYP2J2-selective inhibitor and 11,12-EET (100 nmol/L) on MDA-MB-231 cell proliferation. *, $P < 0.05$ versus blank and vehicle; &, $P < 0.05$ versus CYP2J2 inhibitor (5 or 10 μmol/L).

rAAV-CYP2J2 and rAAV-antisense-CYP2J2 infection resulted in long-term induction and repression of CYP2J2 expression, respectively, compared with control (Fig. 2*B*). Importantly, addition of exogenous EETs or rAAV-mediated overexpression of CYP2J2 significantly enhanced MDA-MB-231 cell migration in a Transwell assay (Fig. 2*C* and *D*). Conversely, CYP epoxygenase inhibition with 17-ODYA or rAAV-antisense-CYP2J2 infection decreased MDA-MB-231 cell migration (Fig. 2*C* and *D*).

CYP2J2 expression influences primary tumor size and lung metastases. Uninfected MDA-MB-231 cells (control) or MDA-MB-231 cells infected with rAAV-CYP2J2, rAAV-GFP, or rAAV-antisense-CYP2J2 were injected into mouse mammary glands and allowed to grow for 14 weeks. Xenograft tumor volume was measured every 5 days after cell injection. Mice injected with rAAV-CYP2J2–infected cells showed significantly enhanced tumor growth rate (Fig. 3*A*) and size (Fig. 3*B*) compared with controls ($P < 0.05$). In contrast, tumors in mice injected with rAAV-antisense-CYP2J2–infected cells grew slower and remained smaller ($P < 0.05$). In addition, rAAV-CYP2J2–infected tumors appeared earlier (6.4 $\pm$ 1.1 days) and rAAV-antisense-CYP2J2–infected tumors appeared later (11.3 $\pm$ 2.3 days) than uninfected (8.8 $\pm$ 1.8 days) and rAAV-GFP–infected tumors (9.0 $\pm$ 1.2 days; $P < 0.05$). The effects of CYP2J2 overexpression and antisense to CYP2J2 on xenograft tumor growth are similar to that observed in our previous study with other cancer cell lines (9).

At 14 weeks, all animals were sacrificed and lungs were removed to count metastatic tumor colonies. Interestingly, we observed a significant increase in lung metastases in mice injected with the rAAV-CYP2J2–infected MDA-MB-231 cells compared with mice injected with uninfected and rAAV-GFP–infected cells (Fig. 3*D*). In contrast, no metastatic lung colonies were observed in the rAAV-antisense-CYP2J2–infected group (Fig. 3*C*). These results suggest that CYP2J2 overexpression promotes growth and metastasis of breast carcinoma cells *in vivo*.

Capillary vessel counting in and around primary tumors showed that rAAV-CYP2J2 transfection significantly increased MVD, but antisense rAAV-CYP2J2 decreased MVD compared with controls (44.8 $\pm$ 6.2/HPF in control and 42.8 $\pm$ 6.4/HPF in rAAV-GFP versus 76.8 $\pm$ 9.1/HPF in rAAV-CYP2J2, $P < 0.05$, versus 23.6 $\pm$ 7.3/HPF in antisense rAAV-CYP2J2, $P < 0.05$; Fig. 3*D*). These results suggest that CYP2J2 transfection enhances angiogenesis for primary tumors. To test whether the proliferative effects were due to EET produced by CYP2J2, we conducted the MTT assay under CYP2J2-selective inhibition with or without addition of 11,12-EET (100 nmol/L). The CYP2J2 inhibitor significantly attenuated MDA-MB-231 cell proliferation, but this inhibitory effect was completely reversed by addition of 11,12-EET (Fig. 3*E*). This suggests that CYP2J2-derived EETs mediated MDA-MB-231 cell proliferation.

CYP2J2 expression influences metastases independent of primary tumor growth. To minimize possible effects of differential primary tumor growth rates on lung metastases, additional experiments were done. Uninfected or rAAV-infected MDA-MB-231 cells were injected into mouse mammary pads as before and xenograft tumors were allowed to grow up to a similar size ($\sim$2.5 cm^3; Fig. 4*A*) and weight ($\sim$2 g; Fig. 4*B*), at which time animals were sacrificed to count lung metastases. In this experiment, as before, CYP2J2 overexpression was associated with significantly increased lung metastases (Fig. 4*C*).

In separate experiments, mice received tail vein injection of uninfected or rAAV-infected MDA-MB-231 cells, which were allowed to grow for 4 weeks before mice were sacrificed to determine extent of lung metastases. In this model, CYP2J2 overexpression also led to significantly more lung metastases than control (Fig. 4*D*). Additional metastases were found only in the CYP2J2-transfected group. Two animals had liver metastatic lesions (12 and 9 metastatic foci, respectively), whereas another animal had one lesion in bladder. Together, these experiments indicate that CYP2J2 overexpression promotes increased primary tumor metastatic potential independent of its effects on primary tumor growth.

CYP2J2-derived EETs promote soft agar colony formation and adhesion to fibronectin. The metastatic potential of cancer cells was assessed *in vitro* by their ability to form anchorage-independent colonies in soft agar. MDA-MB-231 cells infected with rAAV-CYP2J2 showed a significant increase in anchorage-independent growth compared with uninfected cells and cells infected with rAAV-GFP. Thus, rAAV-CYP2J2–infected cells produced

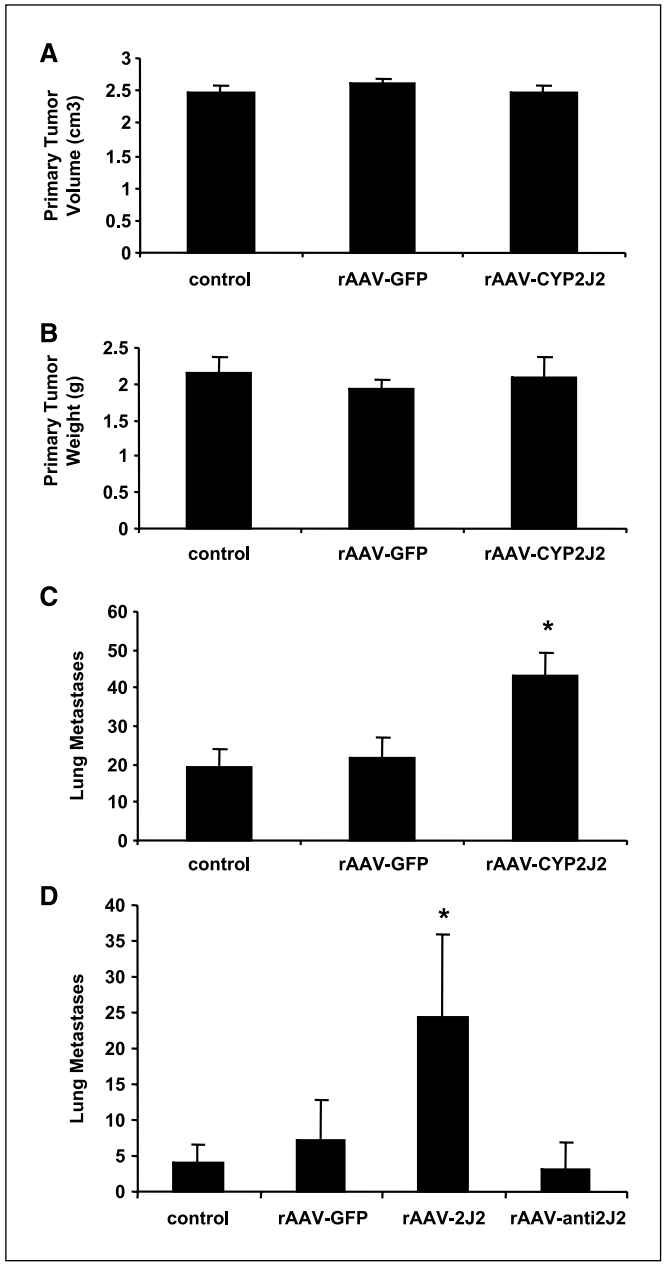

Figure 4. CYP2J2 overexpression promotes lung metastases of xenograft tumors independent of primary tumor size. Mice were injected with uninfected (control) or rAAV-infected MDA-MB-231 cells and primary tumors were measured until volume was 2.5 cm^3, at which time animals were sacrificed. Average volume (*A*) and net weight (*B*) of xenograft tumors for each group at the time of sacrifice. *C,* average number of lung metastases for each group at the time of sacrifice. *D,* uninfected (control) or rAAV-infected MDA-MB-231 cells were injected into tail veins of mice and allowed to grow for 4 to 6 wks. Average numbers of lung metastases for each group. *Columns,* mean; *bars,* SE. *, $P < 0.01$ versus control.

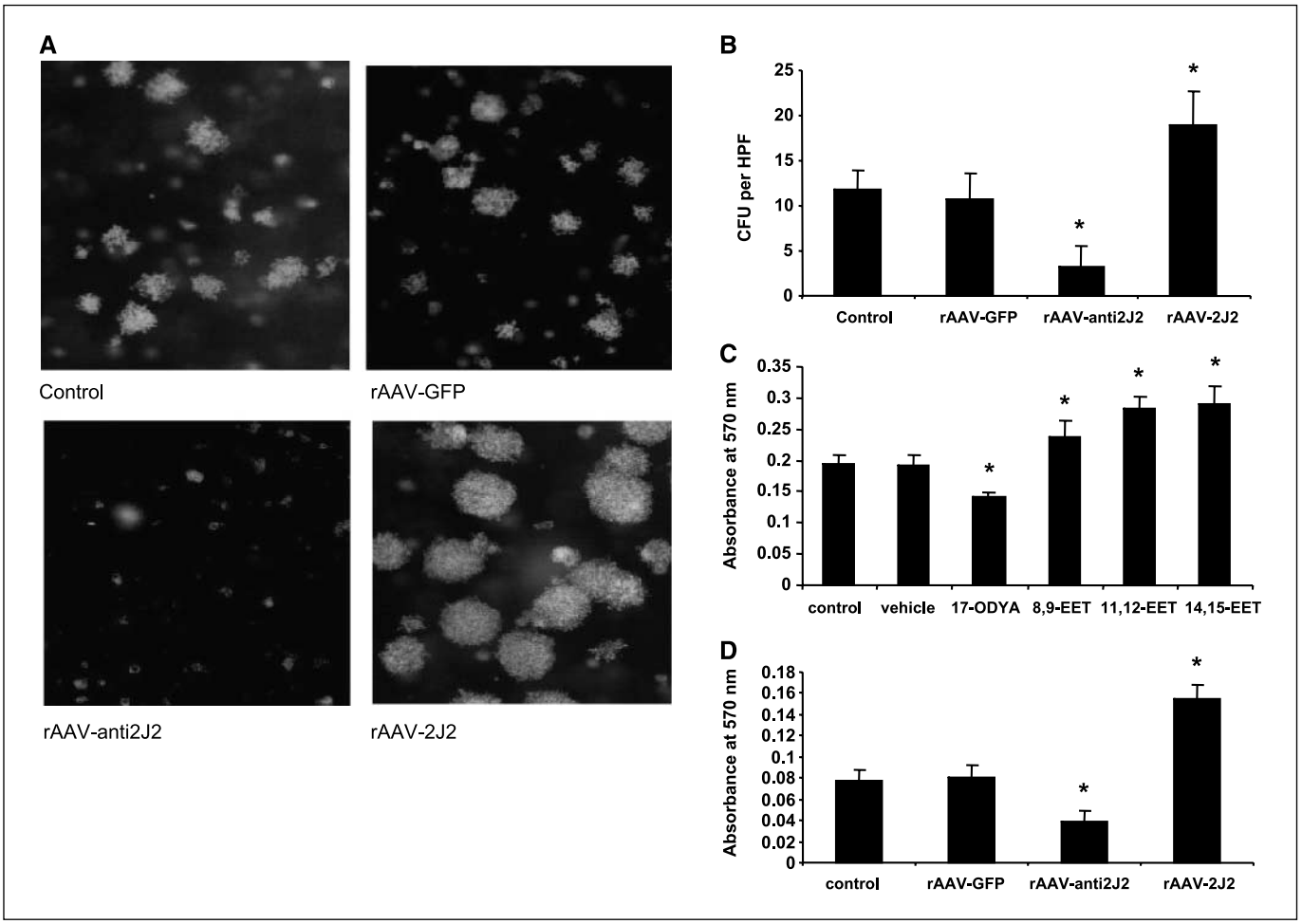

Figure 5. EETs or CYP2J2 overexpression promotes soft agar colony formation and adhesion to fibronectin. *A,* representative photographs of soft agar colony formation of uninfected (control) or rAAV-infected MDA-MB-231 cells. *B,* quantification of soft agar growth of uninfected (control) or rAAV-infected MDA-MB-231 cells. Mean colony number (≥10 cells per colony) per HPF. *C,* mean absorbance value on MTT assay for EET-induced MDA-MB-231 cell adhesion to fibronectin. *D,* mean absorbance value on MTT assay for CYP epoxygenase–induced MDA-MB-231 cell adhesion to fibronectin. *Columns,* mean; *bars,* SE. *, $P < 0.05$ versus control.

larger and more numerous colonies than uninfected or rAAV-GFP–infected cells (Fig. 5*A* and *B*). In contrast, infection with antisense rAAV-CYP2J2 significantly decreased colony size and number (Fig. 5*A* and *B*).

The effect of CYP2J2 expression on adhesion of cancer cells to fibronectin was assessed *in vitro* using a MTT assay. Treatment with EETs (100 nmol/L) increased cell adhesion to fibronectin by 25% to 50% (Fig. 5*C*). Similarly, infection with rAAV-CYP2J2 increased adhesion to fibronectin by ~100% (Fig. 5*D*). In contrast, infection with antisense rAAV-CYP2J2 or treatment with the CYP epoxygenase inhibitor 17-ODYA significantly decreased cancer cell adhesion to fibronectin (Fig. 5*C* and *D*).

CYPCYP2J2 expression influences expression of metastasis-related genes. Cancer metastasis is associated with expression of various molecules, including tetraspanin, MMPs, and E-cadherin, and a variety of cell adhesion molecules. The effect of EETs or CYP epoxygenase overexpression on expression of these metastasis-related genes was examined in MDA-MB-231 cells and in excised tumor xenografts. We found that CYP2J2 overexpression in tumors significantly up-regulated MMP-9 protein expression and activity compared with control (Fig. 6*A*). MMP-2 activity was increased without a corresponding increase in MMP-2 protein expression (Fig. 6*A*). In contrast, antisense rAAV-CYP2J2 infection reduced MMP-9 expression and activity compared with control (Fig. 6*A*). E-cadherin was not detected in these tumors (data not shown). Tumors originating from rAAV-CYP2J2–infected cells also showed increased expression of the prometastatic protein CD44 and decreased expression of antimetastatic proteins CD82 and nm-23 compared with tumors originating from uninfected and rAAV-GFP–infected cells (Fig. 6*B*). In contrast, tumors originating from antisense rAAV-CYP2J2–infected cells showed the reciprocal pattern—diminished CD44 expression and increased CD82 and nm-23 expression (Fig. 6*B*).

Treatment of carcinoma cells in culture with exogenous EETs or infection with rAAV-CYP2J2 led to increased MMP-9 and CD44 expression and decreased CD82 and nm-23 expression (Fig. 6*C* and *D*) and also increased MMP-9 activity (Supplementary Fig. S1). Conversely, infection with antisense rAAV-CYP2J2 or treatment with 17-OYDA had reciprocal effects and resulted in decreased MMP-9 and CD44 expression and increased CD82 and nm-23 expression (Fig. 6*C* and *D*). Together, these results indicate that CYP-derived EETs up-regulate the expression of genes that promote metastasis and down-regulate the expression of genes that may limit metastatic potential.

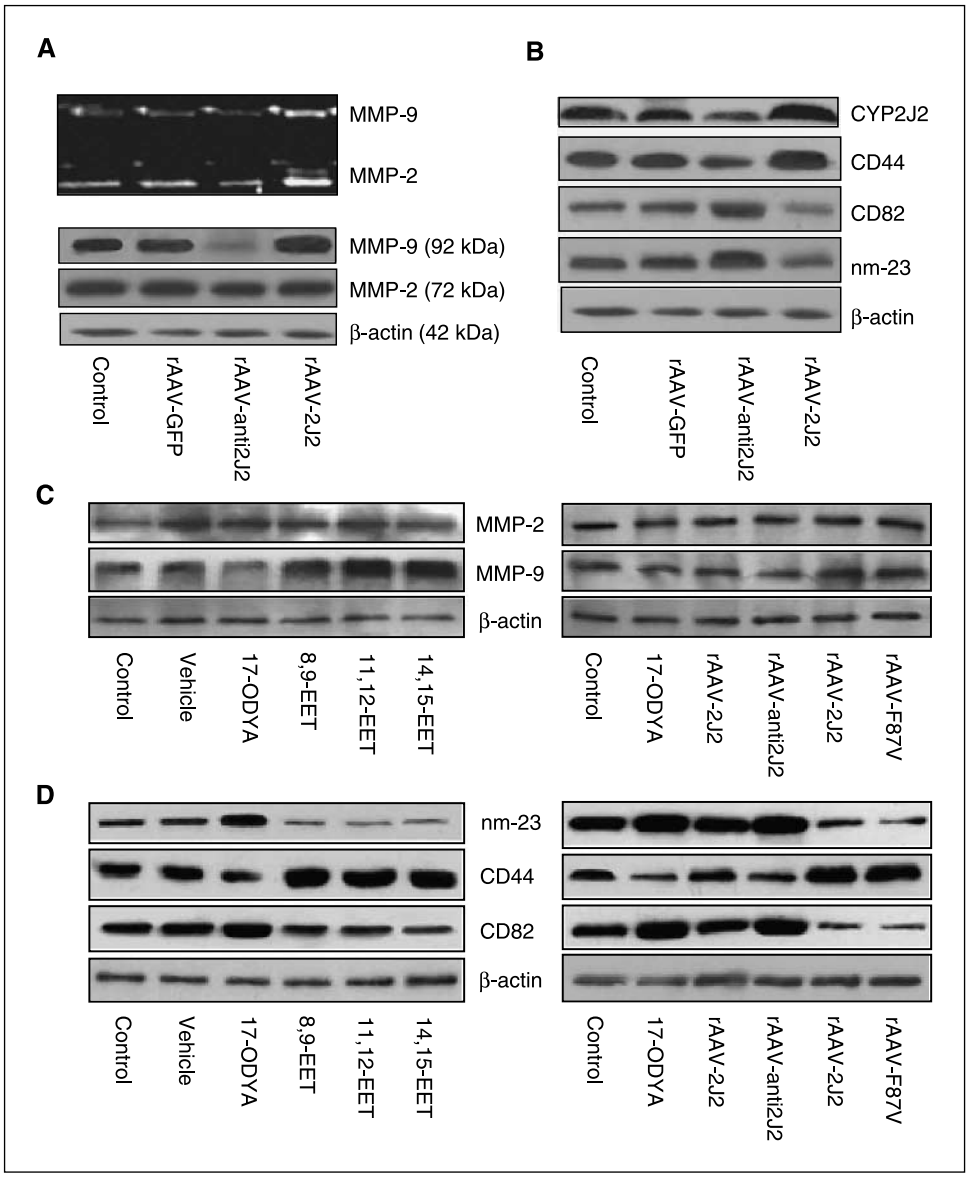

Figure 6. EETs and CYP2J2 overexpression influence expression of metastasis-related genes in xenograft tumors and cancer cells and activity of MMP. *A, top,* gelatinolytic activity of uninfected (control) and rAAV-infected MDA-MB-231 xenograft tumors after 14 wks of growth in mice was analyzed using gelatin zymography. Gelatinolytic activities at sizes corresponding to MMP-2 and MMP-9. *Bottom,* MMP-2, MMP-9, and β-actin protein expression in uninfected and rAAV-infected MDA-MB-231 tumor xenografts. *B,* protein expression levels for CYP2J2, CD44, CD82/KAI-1, nm-23, and β-actin from infected and rAAV-infected MDA-MB-231 tumor xenografts. *C,* MMP-2, MMP-9, and β-actin protein expression levels from MDA-MB-231 cells were treated with vehicle, EETs (100 nmol/L each), and 100 μmol/L 17-ODYA or infected with rAAV-CYP2J2, rAAV-CYP102 F87V, or rAAV-antisense-CYP2J2. *D,* protein expression levels of nm-23, CD82/KAI-1, CD44, and β-actin from EET-treated or rAAV-infected MDA-MB-231 cells.

Finally, we tested whether the EET-induced up-regulation and activation of MMPs played a role in EET-enhanced migration and invasion. Incubation with the nonspecific MMP inhibitor 1,10-phenanthrolin significantly attenuated 11,12-EET–induced migration and invasiveness of MDA-MB-231 cells (Supplementary Fig. S2 and S3). This further suggests that EET-stimulated expression and activity of MMPs may play a role in EET-induced changes in the tumor metastasis phenotype.

Discussion

Tumor metastasis is a multistep process that involves cell proliferation, proteolysis, detachment, adhesion, and migration. The mechanisms underlying each of these steps are complex. CYP2J2-derived EETs seem to promote a prometastatic phenotype at several stages. Our previous study showed that the *P*450 epoxygenase CYP2J2 is abundantly expressed in a variety of human carcinoma cell lines and human tumors. This was shown to have detrimental effects, as overexpression of CYP2J2 or treatment with EETs promoted cell proliferation both *in vitro* and *in vivo* (9). In the current study, we found that, in addition to inducing tumor cell proliferation, both endogenously formed and exogenously applied EETs enhanced tumor cell motility, invasion, adhesion, prometastatic gene expression, and xenograft metastasis to lungs. We also showed that rAAV-mediated CYP2J2 transfection results in a significant increase in EET production and these effects of CYP2J2 on cancer cells are mediated by EETs.

A significant finding is that CYP2J2-derived EETs lead to MMP activation in tumor cells. This can enhance tumor progression or metastases in several ways. In renal epithelial cells, MMP activation is required for EET-induced EGFR activation (22). We recently observed similar effects in carcinoma cell lines and endothelial cells, where CYP epoxygenase–derived EETs were found to significantly enhance phosphorylation of EGFR and activate downstream signaling cascades, including MAPK and PI3K/Akt pathways (5, 9). Such activation has been reported to trigger up-regulation of metastasis-related genes, such as *MMPs* (23) and *CD44* (24, 25), and down-regulation of antimetastatic genes, such

as *CD82/KAI-1* and *nm-23*, and to modulate cancer cell attachment to matrix (25, 26). MMP-2 seems to be critical for tumor enlargement, whereas MMP-9 is critical for stimulating angiogenesis in developing tumors, a process that is also stimulated by EETs (5, 25). Herein, we report that CYP2J2 overexpression or treatment with physiologically relevant concentrations of EETs induces many of these prometastatic changes in carcinoma cells and in tumors.

One potential mechanism for EET activation of MMPs is through induction of plasminogen activators. In this regard, EET treatment or CYP2J2 overexpression in endothelial cells has been shown to induce t-PA expression and activity (7). Plasminogen activators, including t-PA and urokinase-type plasminogen activator, have been widely studied in carcinomas and a high level of plasminogen activator expression is associated with carcinoma metastasis and poor prognosis (27–29). Plasminogen activators convert plasminogen to a proteolytic enzyme called plasmin, which digests fibrin and matrix and promotes MMP maturation (29). Collectively, these data suggest that increased expression and/or activity of t-PA induced by CYP epoxygenase–derived EETs may contribute to human cancer metastasis through activation of MMPs. Additionally, activation of MMPs may enhance cancer cell growth (30), stimulate angiogenesis (31), and also modulate cell adhesion (32, 33). In this study, a MMP inhibitor significantly attenuated 11,12-EET–induced cancer cell migration and invasiveness, which further supports that the up-regulation and activation of MMPs by EETs contribute to CYP2J2-enhanced metastasis.

CYP epoxygenase overexpression or addition of EETs increased cell adhesion to fibronectin and lung colonization of carcinoma cells following tail vein injection. This suggests that EETs may promote a prometastatic phenotype in tumor cells that is distinct from effects on primary tumor growth. We found that CD44 is also up-regulated in tumor cells by CYP epoxygenases or EETs. As with MMPs, increased CD44 expression can contribute to a metastatic phenotype in several ways. CD44 is an adhesion molecule with binding domains for the extracellular matrix component hyaluronic acid. CD44-mediated adhesion also leads to signaling events involving transmembrane and cytoplasmic tail domains that may enhance cancer cell detachment, motility, matrix degradation, and metastases (34, 35). In addition, the extracellular glycoprotein domains of CD44 can bind growth factors, cytokines, and enzymes to concentrate the activities of these molecules near the cell surface. Finally, CD44 expression can activate NF-κB signaling (36), which could further promote cancer metastasis by up-regulating a variety of prometastatic genes.

CD82/KAI-1 is a transmembrane glycoprotein member of the transmembrane-4 superfamily (tetraspanin), which has inhibitory effects on tumor cell motility and metastasis. Studies have found that loss of CD82 expression is correlated with increased tumor metastases and poor prognosis in a variety of human carcinomas (37–41). In contrast, CD82 expression is associated with improved prognosis through inhibition of cancer metastasis (37, 42). CD82 has been implicated in the assembly of integrin-containing signaling complexes, thus modulating the function of integrin receptors in cell migration (43). CD82 down-regulates cell surface expression and signaling from EGFRs and α_6 integrins, which decreases cellular adhesion and morphogenesis (44, 45). EET treatment and CYP epoxygenase overexpression markedly reduced CD82 protein expression, whereas CYP epoxygenase inhibition or down-regulation of CYP2J2 significantly up-regulated CD82 expression in both cancer cell lines and MDA-MB-231 cell xenografts. Thus, down-regulation of CD82 by CYP epoxygenase–derived EETs may promote the metastatic phenotype observed in these studies.

Although *nm-23* was identified as a cancer metastasis suppressor gene almost 2 decades ago (46, 47), the biochemical pathway by which elevated nm-23 expression suppresses metastasis is still unclear. Our work showed that EET incubation with cultured cancer cells and CYP epoxygenase overexpression down-regulated nm-23. Together, these studies suggest that CYP epoxygenase–derived EETs promote human carcinoma metastasis at least partially through down-regulating expression of nm-23 and CD82.

In conclusion, our findings suggest that CYP2J2-derived EETs may play important roles in promoting invasion and metastasis of human cancers through several mechanisms. EETs activate many signaling pathways that can have both short-term (cell motility, invasion, and adhesion) and long-term (gene expression) effects on carcinoma cells. The effects of CYP2J2-derived EETs may involve down-regulation of metastatic suppressor genes, up-regulation of metastatic enhancing genes, and activation of a variety of signaling cascades, such as PI3K/Akt and MAPK. These findings, combined with previous data (9), suggest that inhibition of CYP epoxygenases and EET pathways could represent a novel therapeutic strategy for the treatment of human carcinomas.

Acknowledgments

Received 9/30/2006; revised 5/2/2007; accepted 5/10/2007.

Grant support: National Nature Science Foundation Committee of China (No. 30430320 and 30340067), National "973" projects (No. 2006CB503801 and 2005DFA30880), and Intramural Research Program of the NIH, National Institute of Environmental Health Sciences.

The costs of publication of this article were defrayed in part by the payment of page charges. This article must therefore be hereby marked *advertisement* in accordance with 18 U.S.C. Section 1734 solely to indicate this fact.

References

1. Capdevila JH, Falck JR, Harris RC. Cytochrome P450 and arachidonic acid bioactivation. Molecular and functional properties of the arachidonate monooxygenase. J Lipid Res 2000;41:163–81.
2. Cohen RA, Vanhoutte PM. Endothelium-dependent hyperpolarization: beyond nitric oxide and cyclic GMP. Circulation 1995;92:3337–49.
3. Node K, Huo Y, Ruan X, et al. Anti-inflammatory properties of cytochrome P450 epoxygenase-derived eicosanoids. Science 1999;285:1276–9.
4. Wang H, Lin L, Jiang J, et al. Up-regulation of endothelial nitric-oxide synthase by endothelium-derived hyperpolarizing factor involves mitogen-activated protein kinase and protein kinase C signaling pathways. J Pharmacol Exp Ther 2003;307:753–64.
5. Wang Y, Wei X, Xiao X, et al. Arachidonic acid epoxygenase metabolites stimulate endothelial cell growth and angiogenesis via MAP kinase and PI3 kinase/Akt signaling pathways. J Pharmacol Exp Ther 2005;314:522–32.
6. Yang B, Graham L, Dikalov S, et al. Overexpression of cytochrome P450 CYP2J2 protects against hypoxia-reoxygenation injury in cultured bovine aortic endothelial cells. Mol Pharmacol 2001;60:310–20.
7. Node K, Ruan XL, Dai J, et al. Activation of Gαs mediates induction of tissue-type plasminogen activator gene transcription by epoxyeicosatrienoic acids. J Biol Chem 2001;276:15983–9.
8. Seubert J, Yang B, Bradbury JA, et al. Enhanced postischemic functional recovery in CYP2J2 transgenic hearts involves mitochondrial ATP-sensitive K^+ channels and p42/p44 MAPK pathway. Circ Res 2004;95:506–14.
9. Jiang J-G, Chen C-L, Card JW, et al. Cytochrome P450 2J2 promotes the neoplastic phenotype of carcinoma cells and is up-regulated in human tumors. Cancer Res 2005;65:4707–15.
10. King LM, Ma J, Srettabunjong S, et al. Cloning of CYP2J2 gene and identification of functional polymorphisms. Mol Pharmacol 2002;61:840–52.
11. Wang HLL, Jiang J, Wang Y, et al. Up-regulation of endothelial nitric-oxide synthase by endothelium-derived hyperpolarizing factor involves mitogen-activated

protein kinase and protein kinase C signaling pathways. J Pharmacol Exp Ther 2003;307:753–64.
12. Wang T, Li H, Zhao C, et al. Recombinant adeno-associated virus-mediated kallikrein gene therapy reduces hypertension and attenuates its cardiovascular injuries. Gene Ther 2004;11:1342–50.
13. Fishman DA, Liu Y, Ellerbroek SM, Stack MS. Lysophosphatidic acid promotes matrix metalloproteinase (MMP) activation and MMP-dependent invasion in ovarian cancer cells. Cancer Res 2001;61:3194–9.
14. Bajo AM, Schally AV, Krupa M, Hebert F, Groot K, Szepeshazi K. Bombesin antagonists inhibit growth of MDA-MB-435 estrogen-independent breast cancers and decrease the expression of the ErbB-2/HER-2 oncoprotein and c-jun and c-fos oncogenes. Proc Natl Acad Sci U S A 2002;99:3836–41.
15. Richert MM, Phadke PA, Matters G, et al. Metastasis of hormone-independent breast cancer to lung and bone is decreased by α-difluoromethylornithine treatment. Breast Cancer Res 2005;7:R819–27.
16. Weidner NSJ, Welch WR, Folkman J. Tumor angiogenesis and metastasis-correlation in invasive breast carcinoma. N Engl J Med 1991;324:1–8.
17. Lafite PDS, Buisson D, Macherey AC, Zeldin DC, Dansette PM, Mansuy D. Design and synthesis of selective, high-affinity inhibitors of human cytochrome P450 2J2. Bioorg Med Chem Lett 2006;16:2777–80.
18. Li Y, Bhuiyan M, Alhasan S,. Senderowicz AM, Sarkar FH. Induction of apoptosis and inhibition of c-erbB-2 in breast cancer cells by flavopiridol. Clin Cancer Res 2000; 5:223–9.
19. Chernicky CL, Yi L, Tan H, Gan SU, Ilan J. Treatment of human breast cancer cells with antisense RNA to the type I insulin-like growth factor receptor inhibits cell growth, suppresses tumorigenesis, alters the metastatic potential, and prolongs survival *in vivo*. Cancer Gene Ther 2000;7:384–95.
20. Zipin A, Israeli-Amit M, Meshel T, et al. Tumor-microenvironment interactions: the fucose-generating FX enzyme controls adhesive properties of colorectal cancer cells. Cancer Res 2004;64:6571–8.
21. Welch DR. Technical considerations for studying cancer metastasis *in vivo*. Clin Exp Metastasis 1997;15: 272–306.
22. Chen J-K, Capdevila J, Harris RC. Heparin-binding EGF-like growth factor mediates the biological effects of P450 arachidonate epoxygenase metabolites in epithelial cells. Proc Natl Acad Sci U S A 2002;99:6029–34.
23. Murai T, Miyauchi T, Yanagida T, Sako Y. Epidermal growth factor-regulated activation of Rac GTPase enhances CD44 cleavage by metalloproteinase disintegrin ADAM10. Biochem J 2006;395:65–71.
24. Zhang M, Wang MH, Singh RK, Wells A, Siegal GP. Epidermal growth factor induces CD44 gene expression through a novel regulatory element in mouse fibroblasts. J Biol Chem 1997;272:14139–46.
25. Zhang M, Singh RK, Wang MH, Wells A, Siegal GP. Epidermal growth factor modulates cell attachment to hyaluronic acid by the cell surface glycoprotein CD44. Clin Exp Metastasis 1996;14:268–76.
26. Tsatas D, Kanagasundaram V, Kaye A, Novak U. EGF receptor modifies cellular responses to hyaluronan in glioblastoma cell lines. J Clin Neurosci 2002;9:282–8.
27. Han B, Nakamura M, Mori I, Nakamura Y, Kakudo K. Urokinase-type plasminogen activator system and breast cancer [review]. Oncol Rep 2005;14:105–12.
28. Gradishar WJ. The future of breast cancer: the role of prognostic factors. Breast Cancer Res Treat 2005;89: S17–26.
29. Duffy M. The urokinase plasminogen activator system: role in malignancy. Curr Pharm Des 2004;10: 39–49.
30. Tester AM, Waltham M, Oh SJ, et al. Pro-matrix metalloproteinase-2 transfection increases orthotopic primary growth and experimental metastasis of MDA-MB-231 human breast cancer cells in nude mice. Cancer Res 2004;64:652–8.
31. Ray JM, Stetler-Stevenson WG. The role of matrix metalloproteases and their inhibitors in tumour invasion, metastasis and angiogenesis. Eur Respir J 1994;7: 2062–72.
32. Kleiner DE, Stetler-Stevenson WG. Matrix metalloproteinases and metastasis. Cancer Chemother Pharmacol 1999;43:S42–51.
33. Deryugina EI, Quigley JP. Matrix metalloproteinases and tumor metastasis. Cancer Metastasis Rev 2006;25: 9–34.
34. Marhaba R, Zoller M. CD44 in cancer progression: adhesion, migration and growth regulation. J Mol Histol 2004;35:211–31.
35. Nagano O, Saya H. Mechanism and biological significance of CD44 cleavage. Cancer Sci 2004;95:930–5.
36. Fitzgerald KA, Bowie AG, Skeffington BS, O'Neill LAJ. Ras, protein kinase Cζ, and IκB kinases 1 and 2 are downstream effectors of CD44 during the activation of NF-κB by hyaluronic acid fragments in T-24 carcinoma cells. J Immunol 2000;164:2053–63.
37. Adachi M, Taki T, Ieki Y, Huang C, Higashiyama M, Miyake M. Correlation of KAI1/CD82 gene expression with good prognosis in patients with non-small cell lung cancer. Cancer Res 1996;56:1751–5.
38. Adachi M, Taki T, Konishi T, Huang CI, Higashiyama M, Miyake M. Novel staging protocol for non-small-cell lung cancers according to MRP-1/CD9 and KAI1/CD82 gene expression. J Clin Oncol 1998;16:1397–406.
39. Lombardi DP, Geradts J, Foley JF, Chiao C, Lamb PW, Barrett JC. Loss of KAI1 expression in the progression of colorectal cancer. Cancer Res 1999;59:5724–31.
40. Sho M, Adachi M, Taki T, et al. Transmembrane 4 superfamily as a prognostic factor in pancreatic cancer. Int J Cancer 1998;79:509–16.
41. Huang C-l, Kohno N, Ogawa E, Adachi M, Taki T, Miyake M. Correlation of reduction in MRP-1/CD9 and KAI1/CD82 expression with recurrences in breast cancer patients. Am J Pathol 1998;153:973–83.
42. Zhang XA, Lane WS, Charrin S, Rubinstein E, Liu L. EWI2/PGRL associates with the metastasis suppressor KAI1/CD82 and inhibits the migration of prostate cancer cells. Cancer Res 2003;63:2665–74.
43. Maecker H, Todd S, Levy S. The tetraspanin superfamily: molecular facilitators. FASEB J 1997;11: 428–42.
44. He B, Liu L, Cook GA, Grgurevich S, Jennings LK, Zhang XA. Tetraspanin CD82 attenuates cellular morphogenesis through down-regulating integrin α6-mediated cell adhesion. J Biol Chem 2005;280:3346–54.
45. Odintsova E, Sugiura T, Berditchevski F. Attenuation of EGF receptor signaling by a metastasis suppressor, the tetraspanin CD82/KAI-1. Curr Biol 2000;10:1009–12.
46. Steeg PS, Bevilacqua G, Kopper L, et al. Evidence for a novel gene associated with low tumor metastatic potential. J Natl Cancer Inst 1988;80:200–4.
47. Ouatas T, Salerno M, Palmieri D, Steeg PS. Basic and translational advances in cancer metastasis: Nm23. J Bioenerg Biomembr 2003;35:73–9.

Cytochrome *P*450 Epoxygenase Promotes Human Cancer Metastasis

Jian-Gang Jiang, Yao-Gui Ning, Chen Chen, et al.

Cancer Res 2007;67:6665-6674.